

YALE PEABODY MUSEUM

P.O. BOX 208118 | NEW HAVEN CT 06520-8118 USA | PEABODY.YALE. EDU

JOURNAL OF MARINE RESEARCH

The *Journal of Marine Research*, one of the oldest journals in American marine science, published important peer-reviewed original research on a broad array of topics in physical, biological, and chemical oceanography vital to the academic oceanographic community in the long and rich tradition of the Sears Foundation for Marine Research at Yale University.

An archive of all issues from 1937 to 2021 (Volume 1–79) are available through EliScholar, a digital platform for scholarly publishing provided by Yale University Library at <https://elischolar.library.yale.edu/>.

Requests for permission to clear rights for use of this content should be directed to the authors, their estates, or other representatives. The *Journal of Marine Research* has no contact information beyond the affiliations listed in the published articles. We ask that you provide attribution to the *Journal of Marine Research*.

Yale University provides access to these materials for educational and research purposes only. Copyright or other proprietary rights to content contained in this document may be held by individuals or entities other than, or in addition to, Yale University. You are solely responsible for determining the ownership of the copyright, and for obtaining permission for your intended use. Yale University makes no warranty that your distribution, reproduction, or other use of these materials will not infringe the rights of third parties.



This work is licensed under a Creative Commons Attribution-NonCommercial-ShareAlike 4.0 International License.
<https://creativecommons.org/licenses/by-nc-sa/4.0/>



Objective analysis of the upwelling ecosystem off Baja California

by Dong-Ping Wang¹ and John J. Walsh²

ABSTRACT

The method of empirical orthogonal function (EOF) analysis is applied to nutrient data of hydrostations and surface maps to study the temporal and spatial structures of the major processes in the upwelling ecosystem off Baja California, during the 1972 MESCAL I experiment. It is demonstrated that the EOF analysis leads to a meaningful separation of the uptake process from the dominant conservative processes. In the interior, the upwelling ecosystem was characterized by isentropic flow and the uptake of phosphate and nitrate by the downward migrating dinoflagellates. At the surface, while the general background showed alongshore quasi-steady band structures, there appeared distinct, temporally variable patches of upwelled water. Evidence suggests that the transition from "new" patches of high nutrient but low fluorescence concentrations to "old" patches of low nutrient but high fluorescence concentrations is induced mainly by the local decay of upwelling circulation.

1. Introduction

Most frequently observed along the west coasts of continents in the mid- and tropical latitudes, coastal upwelling is generally characterized by the appearance of shoreward, upsloping isopycnals in the interior and a narrow band of relatively cold water at the surface. This "anomalous" horizontal density distribution is believed to be induced by the upward (and shoreward) interior flow necessary to compensate for the loss of offshore surface Ekman transport driven by the prevailing equatorward wind. The biological effect of this upward water movement is to bring the rich nutrients from the interior into the euphotic surface layer where photosynthesis can take place as the nutrients become available to phytoplankton. Consequently, coastal upwelling areas are generally associated with high primary productivity and high fish yields. It is estimated that one-half of the ocean's fish catches are obtained in the coastal upwelling areas which comprise only 0.1% of the world ocean's surface area (Cushing, 1969)

1. Chesapeake Bay Institute, The Johns Hopkins University, Baltimore, Maryland, 21218, U.S.A.

2. Oceanographic Sciences Division, Brookhaven National Laboratory, Upton, New York, 11973, U.S.A.

An upwelling ecosystem model was constructed (Walsh, 1975) to simulate the complex interactions among nutrient supply (upward water movement), dispersion (water mixing and offshore water drift), consumption (uptake), and internal regeneration (herbivore excretion). Also included in this model are the effects of the diel cycle of photosynthesis, the self-shading by phytoplankton of light penetration, and the diel migration, and the grazing stress of the herbivores. Although it is admittedly crude, Walsh's model does seem able to incorporate both the important physical and biological processes in the upwelling ecosystem, and it agrees reasonably well with some of the independent observations taken along a drogue track. On the other hand, to compare the model's results with the drogue track stations, an assumption has to be made on the nature of the water circulation; i.e., a steady state, 2-dimensional (axis along the direction of surface flow) x - z circulation pattern is implied. Otherwise, either temporal or horizontal spatial variations will make interpretation of the data rather difficult.

However, neither the steady state nor the 2-dimensional circulation pattern is likely to be generally a valid assumption for the upwelling ecosystem. "Patches" or "plumes" of the surface nutrient and chlorophyll a concentrations are common features of the upwelling ecosystem (Walsh, 1972). Wind and current oscillations on the time scale of the nutrient uptake process (several days) are the characteristic features of the coastal spectrum (Smith, 1974). Hence, both the horizontal spatial and the temporal variations of the physical environment should not be overlooked if the steady state assumption is unrealistic.

In addition to influencing the nutrient supply and dispersion rate, the variable physical environment may have other strong, but subtle, impacts on the biological processes. For example, under a steady state condition of constant yield, the growth rate of phytoplankton is a constant fraction of the nutrient uptake rate, which is a function of the *in situ* (equilibrium) nutrient concentration (Dugdale, 1967). This simple relationship (modeled with the Michaelis-Menton formula) between the phytoplankton uptake rate and the *in situ* nutrient concentration can not be used to account for the uptake process in a transient state (Dugdale, 1975); it has been suggested that instead of depending on the *in situ* nutrient concentration, the growth rate of phytoplankton depends mainly on the "internal" nutrient pool during the transient stage (e.g., Caperon and Meyer, 1972; Grenney, Bella, and Curl, 1973).

To resolve the uncertainty about whether the steady state or the transient state is a better representation of the upwelling ecosystem, it is necessary to examine the structures of the horizontal spatial and temporal variations of the upwelling ecosystem from the least biased field observations. The use of an auto-analyzer, fluorometer, and a shipboard computer system (e.g., Walsh, Kelley, Dugdale, and Frost, 1971) provides daily quasi-synoptic maps of the surface temperature, chlorophyll fluorescence, and nutrient distributions, while an offshore hydro-station transect provides daily interior density and nutrient distributions in a relatively

limited area. Although lacking the temporal resolution necessary for the study of diel variations of biological and physical processes (which may partly be compensated by anchor station time series measurements), the surface maps and the hydrostation transects are by far the richest chemical and biological data sets for the upwelling ecosystem.

To analyze these massive amounts of data, an objective method of analysis, for both efficiency (the analysis method is computer oriented) and minimal ambiguity (all data are processed under the same "rules"), is desired. In this study, we offer the hypothesis that effects of conservative and nonconservative processes are spatially uncorrelated (section 2), which enables us to apply empirical orthogonal function analysis to separate contributions of nonconservative processes from the observed spatial nutrient and chlorophyll *a* distributions (section 3, section 4). Whether this separation (or the analysis method) is meaningful or not is determined with some independent biological measurements which were aimed at a more thorough study of nonconservative processes, but with limited spatial and temporal information. Finally, the implication of results from this analysis on the time dependence of the upwelling ecosystem is discussed with suggestions for improvement of the ecosystem model (section 5).

2. Empirical orthogonal function analysis

The difficulty in the study of nonconservative processes in the ocean comes mainly from the fact that the observed state variable (e.g., nutrients, chlorophyll *a*) distributions are also affected by conservative processes which are independent of the biological activity. In other words, as long as the influence of conservative processes is not negligible, the conventional multivariate regression analyses for the study of nonconservative processes among various state variables are likely to be hazardous (Walsh, 1971). Hence, a more careful analysis which enables the separation of nonconservative contributions from the observed state variable distributions is needed.

The method of empirical orthogonal function (EOF) analysis,* originated for statistical weather forecasting (Lorenz, 1956), was applied to the study of vertical structures of atmospheric disturbances ("modes") coherent over a large spatial network (Holmström, 1963). The major disturbances can be isolated from the general background by utilizing the property that their influences are systematic over most of the observation stations. Furthermore, by assuming that different types of disturbances are spatially uncorrelated, the observed spatial weather variability usually can be explained in terms of a set of normal "modes" (each mode corresponds to one type of disturbance), which may represent the effects of separable physical

* The EOF analysis is known as principal component analysis in statistics (Cooley and Lohnes, 1971). However, the approach we adopted here follows closely the spirit of EOF analysis as pioneered by Lorenz (1956) in meteorology.

processes. Analogously, by hypothesizing that the spatial "patterns" of different processes are uncorrelated over a sufficiently large area, the major patterns ("normal modes") of spatial state variable distributions can be separated from the general background and may represent the effects of different conservative and non-conservative processes.

More precisely, if $\{u_i(x,y), i = 1, N\}$ is a set of spatial distribution of N different state variables, each state variable distribution can be decomposed into a set of normal modes (patterns), $\{z_j(x,y), j = 1, N\}$

$$u_i(x,y) = \sum_{j=1}^N e_{ij} z_j(x,y), (i, j = 1, N) \quad (1)$$

such that $\langle z_i(x,y) z_j(x,y) \rangle = 0$ if $i \neq j$ and where $\langle \rangle$ is the ensemble average over all spatial observations [for the convenience of the correlation calculation, the $\{u_i(x,y)\}$ are normalized representations of the spatial series; i.e., the original data sets are adjusted to zero mean value and unit variance—no log transformation of the original data has been made (Walsh, 1971)].

The matrix $\{e_{ij}, (i, j = 1, N)\}$ is formed by the i -th element of the j -th eigenvector of the correlation matrix $U_{ij} \equiv \langle u_i(x,y) u_j(x,y) \rangle$,

$$\sum_k U_{ik} e_{km} = \lambda_m e_{im} \quad (2)$$

where λ_m is the eigenvalue of the m -th eigenvector (for convenience, the index of the eigenvector is ordered so that the corresponding eigenvalues are ordered in decreasing magnitude: $\lambda_1 > \lambda_2 \dots > \lambda_N$).

Several properties of the EOF analysis can be derived (Wallace and Dickinson, 1972):

- a. The spatial distribution of each state variable can be decomposed into a set of normal modes (Eq. 1) which may be related to the conservative and non-conservative processes.
- b. The variance explained by each normal mode is equal to the corresponding eigenvalue,

$$\langle z_i(x,y) z_i(x,y) \rangle = \lambda_i \quad (3)$$

Since the $\{\lambda_i\}$ are ordered in descending order, the significance of each mode's contribution to the total variance (of spatial variations) is diminishing with higher mode number. Consequently, only the leading several modes are relevant to the conservative and nonconservative processes; and the "noise" (defined as the nonsystematic variations with respect to the state variables' network) of the system can be identified with the higher modes.

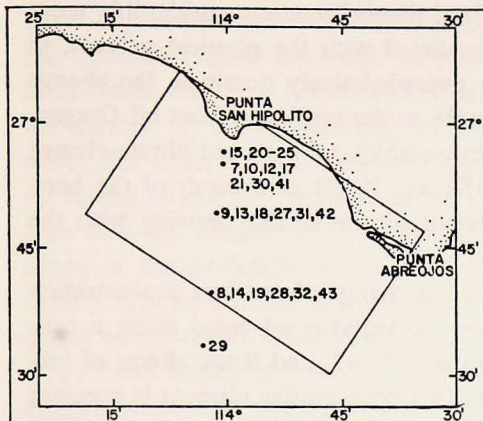


Figure 1. Hydro-station locations for MESCAL I (only transect stations are shown).

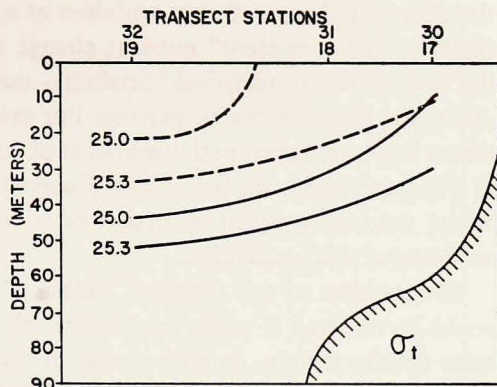


Figure 2. Temporal variations of density surface (solid line: March 14; dotted line: March 19).

- c. The "projection" of the i -th state variable on the j -th normal mode, which measures the significance of the contribution to j -th mode by the i -th state variable, is

$$\frac{\langle u_i(x,y) z_j(x,y) \rangle^2}{\langle z_j^2(x,y) \rangle} = \lambda_j e_{ij}^2 \quad (4)$$

Hence, for each mode (or process), only those state variables with projections significantly different from zero are influenced and interrelated by this same process.

In summary, with the EOF analysis, we are not only able to isolate each significant process governing the spatial distributions of state variables (properties A and B), but we are also able to "identify" each process from the interrelationships among relevant state variables of the corresponding normal mode (property c).

3. Analysis of the interior field

During the two-week (March 1972) MESCAL I cruise off Baja California (Fig. 1), the upwelling ecosystem was in a spin-up phase (Walsh, *et al.*, 1974). Temporal variations of the internal density field are shown in Fig. 2 for two repeated onshore transects taken five days apart. The strengthening of the upwelling between the two transects is clearly reflected in the characteristic upward movements of constant density surfaces.

Because of the temporally variable physical environment, the interpretation of

the observed change of state variables at a fixed depth becomes considerably more difficult. The "apparent" nutrient change associated with the physical process, in the case of strong temporal variability, may overwhelmingly dominate the change due to the nonconservative process. For example, at the upwelling front off Oregon, where there are large spatial gradients of state variables, an apparent nitrate change of $10\mu\text{gat/l}$ within six hours was observed (Kelley, 1975) as a result of the horizontal (and/or vertical) excursion of a constant nitrate surface moving with the semidiurnal tidal oscillation.

The problem of this temporal "aliasing" of the change of nutrient concentration could be resolved if water (and hence, all the nutrients) is advected along a constant density surface. In such a case of "isentropic flow," and if the effects of turbulent mixing are negligible, the concentration of a conservative element is constant

along the isentropic surface. In other words, there is a well-defined functional relationship between density and the conservative element, which allows for the transformation of spatial state variable distributions into the "density coordinate" to eliminate the apparent concentration change due to the movement of constant density surfaces.

Among the various nutrients in the 1972 water column off Baja California, silicate was the conservative element because it is apparently not utilized by the dinoflagellate *Gonyaulax polyedra*, which was the dominant phytoplankton species during the period of observation (Walsh, *et al.*, 1974). Hence, silicate should be highly correlated with the density if the isentropic flow hypothesis is a sensible assumption. This is indeed the case as is demonstrated by the striking linear relationship (Fig. 3) between silicate and density from all data taken along the transect during

the whole cruise. Consequently, the isentropic flow, which has been suggested for the upwelling circulation pattern (e.g., Mooers, *et al.*, 1976), is the dominant circulation feature in this system.

While the scatter around the linear dependence between silicate and density may be merely the random measurement error (Fig. 3), a systematic discrepancy from the

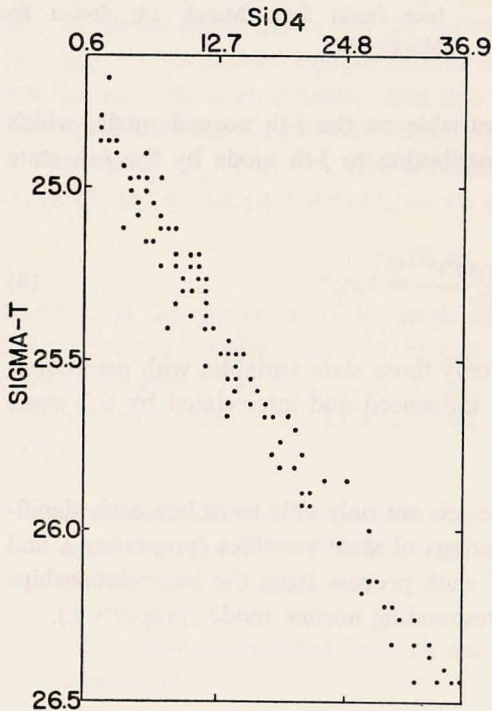


Figure 3. Silicate concentrations vs. sigma-t for all hydro-stations.

linear dependence between density and the nonconservative elements, on the other hand, could be an indication of the effects of nonconservative processes. For example, nitrate was taken up by the phytoplankton; and its relation with the density (Fig. 4) clearly shows a nitrate-deficit in the lighter density regions (inshore and upper regions) where uptake is likely to occur.

To make quantitative separation between the advective process and the uptake process, it is instructive to examine the "appropriate" density range first. For example, during a 1974 study of upwelling off Northwest Africa, an r^2 of 0.90 was observed for density and nitrate at all depths (127 observations) of a 36-hour anchor station study in 700 m of water, in contrast to 0.40 for all station data (426 observations) taken on the shelf. In the upper mixed layer off Baja California, where the isentropic hypothesis is not satisfied, the hydro-station data ($\sigma_t < 25.0$) are discarded for the isentropic analysis. At the off-shore stations, there exist density surfaces at depth which do not enter the inshore region. Hence, the hydro-station data for $\sigma_t > 26.0$ are also excluded from the analysis to avoid the possible bias by these stations. The remaining eighty hydro-cast samples spanning the 2-week period of MESCAL I are then used to compute the correlation matrix among density, temperature, phosphate, nitrate, and silicate (Table 1).

The very high correlation (> 0.94) between density and individual nutrients re-

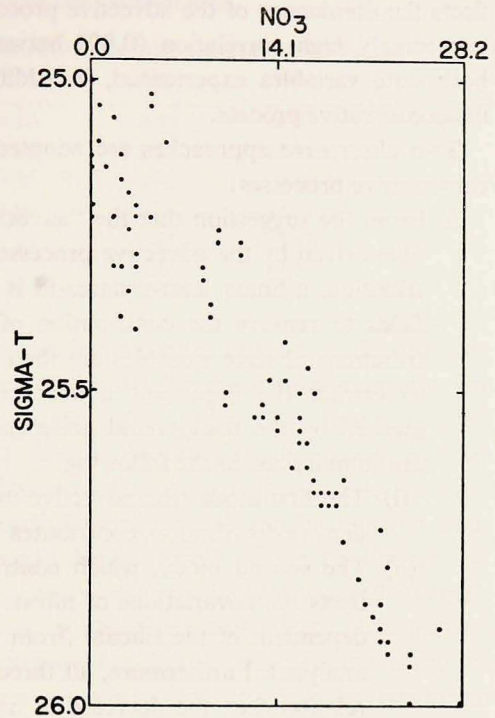


Figure 4. Nitrate concentrations vs. sigma-t for hydro-stations in the density band (25.0-26.0).

the hydro-station data ($\sigma_t < 25.0$) are discarded for the isentropic analysis. At the off-shore stations, there exist density surfaces at depth which do not enter the inshore region. Hence, the hydro-station data for $\sigma_t > 26.0$ are also excluded from the analysis to avoid the possible bias by these stations. The remaining eighty hydro-cast samples spanning the 2-week period of MESCAL I are then used to compute the correlation matrix among density, temperature, phosphate, nitrate, and silicate (Table 1).

The very high correlation (> 0.94) between density and individual nutrients re-

Table 1. Correlation matrix among major state variables in the interior field.

| | σ_t | PO_4 | SiO_4 | NO_3 | T |
|------------|------------|--------|---------|--------|-----|
| σ_t | 1.0 | | | | |
| PO_4 | 0.96 | 1.0 | | | |
| SiO_4 | 0.95 | 0.93 | 1.0 | | |
| NO_3 | 0.94 | 0.99 | 0.91 | 1.0 | |
| T | -0.90 | -0.78 | -0.82 | -0.77 | 1.0 |

flects the dominance of the advective process on the nutrient distribution. Also, the exceedingly high correlation (0.99) between phosphate and nitrate suggests that both state variables experienced, in addition to the advective process, the same nonconservative process.

Two alternative approaches are adopted for the analysis of advective and non-conservative processes:

- a. From the suggestion that the "advective mode" (spatial pattern of state variable driven by the advective processes) can be identified with the density distribution, a linear least-squares-fit is applied to the temperature and nutrient fields to remove the contribution of the advective mode. The residual distributions of state variables are then further examined with the EOF analysis to extract the important nonconservative processes which may be partly masked by the background noise (property B of the EOF analysis) Results are summarized in the following:
 - (i) The first mode (the advective mode), which has the same pattern as the density distribution, contributes 77% of the total variance.
 - (ii) The second mode, which contributes 14.5% of the total variance, reflects the covariations of nitrate, phosphate, and temperature, and is independent of the silicate (from the criterion for property C of the EOF analysis). Furthermore, all three major components show a positive correlation; i.e., the decrease of nitrate is accompanied by the decrease of phosphate and temperature.
 - (iii) The third mode, which contributes 5.6% of the total variance, only shows the variation of silicate. Since there is no correlation with other state variables, the third mode could either be the silicate measurement error, or it could reflect the nonbiological processes (e.g., a sediment transport process).

- b. A direct application of the EOF analysis to the original spatial distribution of the state variables also results in three normal modes which contribute more than 99% of the total variance (Table 2). The notations used in Table 2 (and all the subsequent, similar tables) need some explanation.
 - (i) The first column indicates the mode number; i.e., $\{z_i(x,y), i = 1, 3\}$ denotes the first three modes.
 - (ii) The second column indicates the percentage contributions from each mode to the total variance, per cent variance = $\lambda_i / \sum_{i=1}^5 \lambda_i$, for $z_i(x,y)$.
 - (iii) The matrix elements in the third box are the structure factors of each mode; for example, in Table 2 $z_1(x,y) = 0.46 \sigma_t + 0.46 \text{PO}_4 + 0.45 \text{SiO}_4 + 0.45 \text{NO}_3 - 0.42 \text{T}$, where σ_t , PO_4 , etc., were the spatial distributions measured and normalized.

Table 2. Structures of the three leading eigenmodes from interior data.

| Mode | Total Variance | Modal Amplitude (percent variance in mode) | | | | |
|------|----------------|--|-----------------|------------------|-----------------|-----------------|
| | | σ_t | PO ₄ | SiO ₄ | NO ₃ | T |
| 1 | 91.8 | 0.46 (99.0) | 0.46 (95.6) | 0.45 (93.2) | 0.45 (93.3) | -0.42 (79.6) |
| 2 | 5.8 | -0.09 (—) | 0.35 (4.0) | 0.09 (—) | 0.40 (4.6) | 0.83 (20.0) |
| 3 | 1.8 | 0.0 (—) | -0.21 (—) | 0.85 (6.5) | -0.43 (1.7) | 0.0 (—) |

(iv) Numbers in the bracket underneath the structure factors are the “projections” (section 2) of each state variable on the corresponding mode; for example, in Table 2 $\langle z_1(x,y) \sigma_t(x,y) \rangle^2 / \langle z_1^2(x,y) \rangle \cdot \langle \sigma_t^2(x,y) \rangle = 0.99$.

It is rather encouraging to notice that there is no practical difference between results obtained from the direct EOF analysis and those from the isentropic analysis. The first mode consistently shows the advective process which can be deduced from the fact that all the density variation occurs in the first mode (Table 2). The second mode, which is independent of the two conservative elements (density and silicate), clearly reflects the expected uptake process of phosphate and nitrate. The accompanying decrease of temperature (or increase of salinity) could be the result of entrainment of cold water from below as water moves inshore along the isentropic surface.

The spatial structures of the first and second modes from one transect (which occupied five stations) are shown in Fig. 5 (in this particular case, results are almost identical from either approach). The second mode shows clearly the nitrate (or phosphate) uptake in the inshore upper 30 meters as reflected by the existence of a large concentration gradient along the isopycnal surface. With an estimated 3 cm/

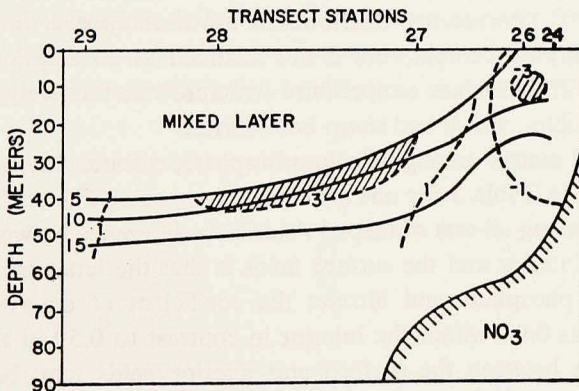


Figure 5. The spatial structures of the first and second normal modes (solid line: first mode; dotted line: second mode).

Table 3. Correlation matrix among major state variables of surface field.

| | SiO ₄ | PO ₄ | NO ₃ | fluor | T |
|------------------|------------------|-----------------|-----------------|-------|-----|
| SiO ₄ | 1.0 | | | | |
| PO ₄ | 0.89 | 1.0 | | | |
| NO ₃ | 0.73 | 0.77 | 1.0 | | |
| fluor | 0.80 | 0.70 | 0.45 | 1.0 | |
| T | -0.77 | -0.55 | -0.46 | -0.75 | 1.0 |

sec onshore flow (corresponding to approximately 10^{-2} cm/sec vertical velocity), the nitrate uptake rate is about $2 \mu\text{gat NO}_3 \text{ l}^{-1} \text{ day}^{-1}$ in the long term mean (in a quasi-steady state), which agrees quite well with the averaged direct nitrate uptake rate measurements (Walsh, *et al.*, 1974). Also, nitrate uptake occurred mainly in the interior of the newly upwelled water, as opposed to the typical uptake process which is confined to the upper photosynthetic layer. This feature is also consistent with earlier observations (Epply, *et al.*, 1968) that dinoflagellates migrate down into the nutrient-rich water to take up nitrate. The significance of this rather unique uptake behavior on the ecosystem will be discussed in the final section.

4. Analysis of the surface field

Surface nutrients, chlorophyll fluorescence, and temperature distributions were mapped extensively over a 20×35 nm rectangular area during the entire period of the MESCAL I cruise. This is by far the richest set of marine ecological data which provides a detailed synoptic view of surface state variable distributions, and is most useful for the study of both the spatial and temporal variations of the upwelling ecosystem.

Six sets of surface maps spanning a nine-day period (March 11-March 19) were employed in this analysis. For each set of surface maps, nutrients (silicate, nitrate, and phosphate) and fluorescence distributions are decomposed into normal modes with the EOF analysis. Temperature is not included as an additional variable because the rather diffuse surface temperature structure was relatively noisy compared to other state variables, which had sharp boundaries.

The correlation matrix among silicate, phosphate, nitrate, fluorescence and temperature is shown in Table 3 for one set of surface maps. (The statistical properties are very similar among all sets of maps.) A striking difference between the statistical properties in the interior and the surface fields is that the latter lacks the high correlation between phosphate and nitrate; the coefficient of determination (r^2) for these variables was 0.98 within the interior in contrast to 0.59 at the surface. This distinct difference between the surface and interior fields may be interpreted as either nitrogen limitation and/or faster remineralization of phosphorus in the surface waters.

The EOF analysis applied to each set of surface nutrients and fluorescence maps effectively explains the original state variable variations with two normal modes. (For each case, in general, more than 90% of the total variance can be explained by the first two modes, Table 4.) The first mode, which shows a positive correlation among all state variables (Table 5), clearly reflects the conservative physical processes (advection and mixing). In other words, the general background of the surface field is the result of the advection and mixing (diffusion) of the "upwelled water" with high nutrients and high fluorescence concentrations. The spatial structure of the first mode (Fig. 6), in general, is characterized by longshore bands with concentration decreasing offshore. This feature is consistent with

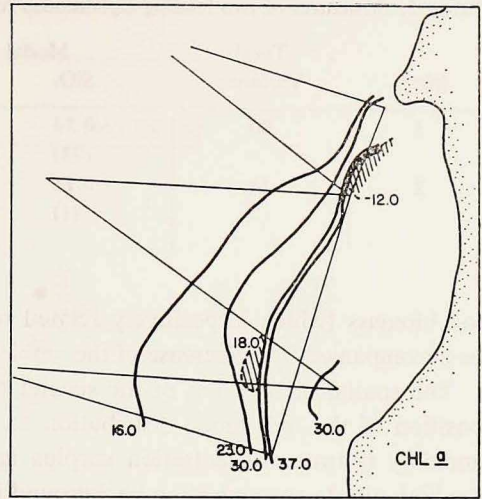


Figure 6. The spatial structures of the first and second normal modes. The zig-zag line is the ship track; the solid line is the first mode structure; the slashed "patches" are the second mode structures (fluorescence units for chlorophyll).

our conceptual upwelling circulation pattern which implies source water upwelled in the inshore region and advected or diffused offshore. The longshore homogeneous concentration distribution is also an expected result of the longshore current effect. With all this supporting evidence, there seems to be little ambiguity in our interpretation of the first mode as the conservative (physical) mode.

The second mode, as suggested by its independence of silicate (Table 5), is likely to reflect certain nonconservative biological processes. This conjecture is further strengthened by the negative correlation between nitrate and fluorescence in the second mode, a feature one would naturally expect for the uptake process. In other words, because of the conservation of nitrogen flow, an increase of the phytoplank-

Table 4. Variance of each state variable explained by the first two eigenmodes.

| Date | SiO ₄ | PO ₄ | NO ₃ | fluor |
|-------|------------------|-----------------|-----------------|-------|
| 3-11* | 94 | 97 | 98 | 98 |
| 3-11 | 91 | 87 | 88 | 94 |
| 3-13 | 94 | 91 | 95 | 95 |
| 3-14 | 96 | 96 | 99 | 97 |
| 3-16 | 87 | 87 | 100 | 96 |
| 3-19 | 93 | 93 | 99 | 90 |

* Day map.

Table 5. Structures of two leading eigenmodes from surface field.

| Mode | Total Variance | Modal Amplitude (percent variance in mode) | | | |
|------|----------------|--|-----------------|-----------------|---------------|
| | | SiO ₄ | PO ₄ | NO ₃ | fluor |
| 1 | 80 | 0.54 (93) | 0.53 (90) | 0.46 (68) | 0.46 (68) |
| 2 | 14 | -0.11 (1) | 0.12 (1) | 0.69 (27) | -0.71 (28) |

ton biomass (which is positively related to the fluorescence concentration) should be accompanied by a decrease of the ambient nitrate concentration.

The spatial distribution of the second mode is shown in Fig. 6 with the superposition of the first mode distribution as the general background. The "positive" anomaly (nitrate concentration surplus and fluorescence concentration deficit) in the high nitrate concentration background is the area (patch) with the highest nitrate but relatively lower fluorescence concentrations. The "negative" anomaly in the low nitrate concentration background is the area (patch) with relatively lower nitrate but very high fluorescence concentrations. The patches of water characterized by the "positive" and "negative" anomalies are generally thought to represent the "new" and "old" stages of upwelled water, with the names "blue water" and "brown water," respectively (Strickland, Eppley, and de Mendiola, 1969). Hence, our suggestion that the second mode reflects the influence of uptake process is consistent with this concept of "new" and "old" upwelled water.

So far, our analysis is limited to showing that the EOF analysis indeed makes a sensible separation of the conservative and the nonconservative processes through a detailed comparison of results from one particular set of data with the conceptual upwelling model. Our approach with the EOF analysis, once its validity (hypothesis) has been

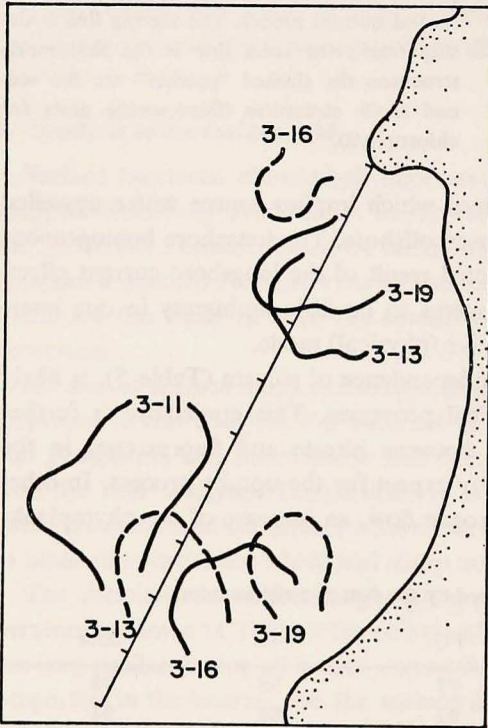


Figure 7. Spatial and temporal distributions of "new" and "old" patches (solid line: "new" patches; dotted line: "old" patches). The nutrient and chlorophyll concentrations are shown in Fig. 8 for the corresponding patches.

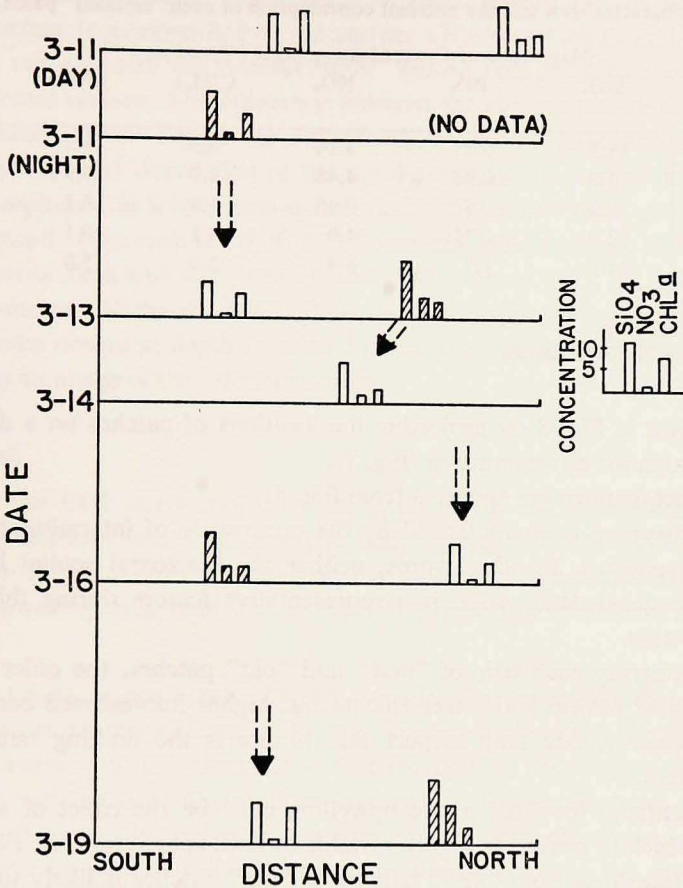


Figure 8. Sequential structures of "new" and "old" patches (concentration is in $\mu\text{g l}^{-1}$ and $\mu\text{g l}^{-1}$ for nutrients and chlorophyll). Blank box: "old" patch; Dashed box: "new" patch.

verified, however, can be applied "objectively" (repeatedly in exactly the same fashion) to all sets of data to generate a much more complete picture of the temporal and spatial structures of an upwelling ecosystem. This advantage of the objective analysis makes it possible to seriously attempt to answer questions on the evolution and the important governing processes of the upwelling ecosystem.

For example, while the distinct high nutrient concentrations in the "blue water" may be good evidence for the "new" upwelled water, the suggestion that the "brown water" is the "old" upwelled water can be confirmed only if the life history of the patches of water can be documented. In Fig. 7, which is a composite picture of all the "anomalies" during the nine-day period, the transition from the "blue water" patch to the "brown water" patch is rather clearly shown. A different view, with emphasis on the properties (silicate, nitrate, and fluorescence concentrations) of the

Table 6. The characteristics and the nutrient consumption of each "isolated" patch.

| Date | Magnitude of Concentration ($\mu\text{g l}^{-1}$ and $\mu\text{g l}^{-1}$) | | | | | $\frac{\Delta\text{PO}_4}{\Delta\text{NO}_3}$ |
|-------|--|-----------------|-----------------|------------------|---------------------|---|
| | SiO ₄ | PO ₄ | NO ₃ | CHL _a | ΔNO_3 | |
| 3-11* | 11.3 | 0.83 | 3.14 | 4.5 | 6.2 | 0.05 |
| 3-13 | 13.0 | 0.96 | 4.46 | 3.7 | 6.9 | 0.05 |
| 3-16† | 9.2 | 0.6 | 0.46 | 5.0 | 6.1 | 0.06 |
| 3-16 | 12.0 | 0.75 | 4.0 | 4.5 | 6.1 | 0.07 |
| 3-19 | 14.5 | 1.1 | 8.4 | 3.0 | 5.0 | 0.06 |

* Data from day map.

† An "old" but "isolated" patch.

patch, is shown in Fig. 8 by projecting the locations of patches on a diagonal line crossing through the upwelling area (Fig. 7).

Two distinct features are apparent from Fig. 8:

- a. The ecosystem is characterized by the occurrence of intermittent, active upwelling patches. In other words, neither the horizontal spatial homogeneity nor the quasi-steady state is a representative feature during this period of observation.
- b. By comparing each pair of "new" and "old" patches, the older always has diminished nitrate and lower silicate but higher fluorescence concentrations. Consequently, one may suspect that nitrate is the limiting nutrient in the ecosystem.

The intermittent, localized active upwelling must be the effect of an upwelling circulation which in general is highly variable in both space and time (Walsh, *et al.*, 1974). The transition from "new" patches to "old" patches is likely to be induced by the shut-off of the nutrient supply from depth as a result of the decay of upwelling circulation. This speculation is supported by the observation that the "old" patch always has relatively lower silicate concentration, which must result from the leveling of an isopycnal surface, because of the conservative property of silicate. The effect of intermittent nutrient supply on the phytoplankton ecology could be very complicated, as we have suggested in the Introduction (section 1).

Interpretation based *only* on the surface fluorescence concentrations is rather difficult because of the vertical migration of the dinoflagellates. Hence, qualitative discussion of the phytoplankton ecology during a period of intensive physical variability is deferred to the last section. The quantitative results for the uptake of non-conservative nutrients, however, can be obtained from a combined knowledge of the surface and interior fields. In the interior (section 3), the nutrient supply is sufficiently well described by the advective mode which assumes a fixed relationship among density, silicate, nitrate, and phosphate. Because silicate was a conservative element during MESCAL I, and because it is reasonable to assume that the high

silicate concentration in the "new" patch of water reflects the intersection of an isopycnal surface (corresponding to the surface silicate concentration) with the sea surface, we can estimate the "conservative" nitrate and phosphate concentrations on the isopycnal surface. The difference between the surface nitrate (or phosphate) and the "conservative" nitrate (or phosphate) concentration represents the total nitrate (or phosphate) deficit due to the uptake process. It is remarkable that the ratios of phosphate deficit to nitrate deficit (Table 6) for all "new" patches of water agree consistently both with the 0.06 ratio estimated independently from the second mode of interior field and with the classical N:P ratio of 15:1 for seawater (Redfield, Ketchum, and Richards, 1963). This, in turn, supports our earlier suggestion that the uptake occurs at depth (section 3), and that the surface nutrient distribution is merely an image of the interior process.

5. Discussion

Based on our EOF analysis of the density, nutrients, and fluorescence data from interior hydrostations and surface maps, and bearing in mind the inherent non-causal nature of any multivariate analysis, the following interpretation can be drawn about the upwelling ecosystem during the 1972 period of the MESCAL I experiment:

- a. *Quasi-steady "mean" state.* In the interior, the "classical" two-dimensional circulation pattern with water flowing shoreward along the isopycnal surfaces is consistent with the observation that the density distribution is highly correlated with nutrient distributions. As nutrients were advected onshore, the bloom of *Gonyaulax polyedra*, the dominant phytoplankton species during the experimental period, evidently migrated downward into the interior (upper 30 meters) to take up phosphate and nitrate in a ratio of $\sim 0.06:1$ with an estimated uptake rate of $\cong 2 \mu\text{gat NO}_3 \text{ l}^{-1}\text{day}^{-1}$. At the surface, the state variable distributions, in general, showed longshore band structures with concentrations decreasing offshore. This characteristic band structure could probably be the result of longshore advection (by the surface current) and offshore diffusion of upwelled "source water" with high nutrients and chlorophyll *a* concentrations. Estimation of the "net" plant biomass production from the surface fluorescence concentration is difficult, however, because of the uncertainty introduced by the vertical migration of the dinoflagellates.
- b. *Horizontal "patchiness."* Strong temporal variability occurred mainly at the several-day time scale which is most likely associated with the low-frequency wind and current fluctuations. On this time scale, the upwelling "center" off Punta San Hipolito appears to induce strong biological activity which results in spatial translation of patches of water with characteristics distinct from their environment. Two types of patchiness are noticeable: the "blue water" with

high nutrient but low fluorescence concentrations, and the "brown water" with low nutrient but high fluorescence concentrations. Evidence suggests that the transition from the "blue water" to the "brown water" patches may be induced by the decay of local upwelling circulation, or equivalently, by the shut-off of nutrient supply; one might expect to observe a continuum between blue and brown water, of course, if the anomaly can persist for one day or longer. Also, the phytoplankton bloom during the transition period appeared to be limited by the nitrate supply, as reflected from the observation that the "brown water" always contained diminished nitrate.

Comparing these results with Walsh's upwelling ecosystem model (Walsh, 1975), the quasi-steady, 2-dimensional "mean" state is consistent with the theory; and hence, the nutrients can be adequately modeled by specifying the appropriate circulation pattern and uptake process. (The production of plant biomass, on the other hand, has to be additionally estimated by assuming grazing and migratory patterns of herbivores and/or phytoplankton; e.g., Fig. 8 of Walsh, *et al.*, 1974.) The transient upwelling patches, however, showed a strong dependence on the variable physical environment, a factor which has not thus far been considered in Walsh's model. The bloom of phytoplankton biomass after the apparent shut-off of nutrient supply is in contradiction to the quasi-steady state theory which assumes an instantaneous, balanced state between the nutrient uptake (proportional to the nutrient supply) and the grazing loss. This contradiction may be resolved by the suggestion of a time lag with the "internal" nitrogen pool playing a significant role in the uptake process during the transient state; and, thus, no obvious functional relationship between the uptake rate and the *in situ* nutrient concentration. Consequently, a deterministic approach to modeling the uptake process during the transient state is not adequate until this intermediate relationship can be more fully documented.

Finally, several comments can be made on the study of the upwelling ecosystem:

- a. With an objective method of analysis (EOF analysis in this study), it becomes possible to deal with massive amounts of surface and interior chemistry data in order to obtain information on the spatial and temporal structures of the upwelling ecosystem. Because of the redundancy of the hydrostation and surface map measurements (both in spatial and in temporal variabilities), the information obtained from the objective analysis should be much more reliable and representative of the upwelling ecosystem than that inferred from discrete (and possibly biased) measurements. Therefore, theoretical work should be oriented toward modeling the results from objective analysis of the hydrostation and surface map measurements, with knowledge partly derived from some independent, suitably designed biological measurements.
- b. The quasi-steady, 2-dimensional model seems able to account for the gross spatial structures of the upwelling ecosystem, which is mainly controlled by

the physical processes. Existent theories, however, fail to explain the temporally variable patches of active upwelling. An outstanding question yet to be answered concerns whether patches are merely "anomalies," whether they play an indispensable role in the upwelling ecosystem, and whether they are mainly of physical or biological origin (Walsh, 1976).

- c. With combined efforts of the objective data analysis which could extract the important information of biological processes from the dominant physical processes, and the theoretical modeling which could single out controlling mechanisms from otherwise complex ecosystems, it seems that the study of "quantitative" biological oceanography (Riley, 1946) is feasible and promising.

Acknowledgments. This study was begun while Mr. Dong-Ping Wang was a summer guest investigator at the Department of Oceanography, University of Washington. Mr. Wang would like to express his appreciation to Dr. C. N. K. Mooers for both his understanding and encouragement. This work was partly supported by National Science Foundation Grants No. GX 33052 to Dr. Mooers at the University of Miami and No. ID072-06422 to Dr. Walsh at the University of Washington, and is a contribution to the IDOE Coastal Upwelling Ecosystems Analysis (CUEA) program.

REFERENCES

- Caperon, J. and J. Meyer, 1972. Nitrogen-limited growth of marine phytoplankton—I. Changes in population characteristics with steady-state growth rate. *Deep-Sea Res.*, 19: 601–618.
- Cooley, W. W. and P. R. Lohenes, 1971. *Multivariate data analysis*. John Wiley & Sons, Inc., 364 pp.
- Cushing, D. H., 1969. Upwelling and fish production. *FAO Fisheries Technical Paper No. 84*, 40 pp.
- Dugdale, R. C., 1969. Nutrient limitation in the sea: dynamics, identification, and significance. *Limnol. Oceanogr.*, 12: 685–695.
- Dugdale, R. C. 1976. Nutrient cycles in the sea, in *The Ecology of the Seas*, D. H. Cushing and J. J. Walsh, eds., Blackwell, Oxford, pp. 141–172.
- Eppley, R. W., O. Holm-Hansen, and J. D. H. Strickland, 1968. Some observations on the vertical migration of dinoflagellates. *J. Phycol.*, 4: 333–340.
- Grenney, W. J., D. A. Bella, and H. C. Curl, 1973. A theoretical approach to interspecific competition in phytoplankton communities. *Amer. Nat.*, 107: 405–421.
- Holmström, I., 1963. On a method for parametric representation of the state of the atmosphere. *Tellus*, 15: 127–149.
- Kelley, J. C., 1975. Time varying distributions of biologically significant variables in the ocean. *Deep-Sea Res.*, 22: 679–688.
- Lorenz, E. N., 1956. Empirical orthogonal functions and statistical weather prediction. *Sci. Rept. No. 1*, Contract AF19(604)–1566, Dept. of Meteorology, M.I.T., 49 pp.
- Mooers, C. N. K., C. A. Collins, and R. L. Smith, 1976. The dynamic structures of the frontal zone in the coastal upwelling region off Oregon. *J. Phys. Oceanogr.*, in press.
- Redfield, A. C., B. H. Ketchum, and F. A. Richards, 1963. The influence of organisms on the composition of sea-water, in *The Sea*, Vol. 2, M. N. Hill, ed., Wiley Interscience, New York, pp. 26–77.

- Riley, G. A., 1946. Factors controlling phytoplankton populations on Georges Bank. *J. Mar. Res.*, 6: 54-73.
- Smith, R. L., 1974. A description of current, wind and sea level variations during coastal upwelling off the Oregon coast, July-August, 1972. *J. Geophys. Res.*, 79: 435-443.
- Strickland, J. D. H., R. W. Eppley, and B. Rojas de Mendiola, 1969. Phytoplankton populations, nutrients, and photosynthesis in Peruvian coastal waters. *Bol. Inst. Mar. Peru-Callao*, 2: 4-45.
- Wallace, J. M. and R. E. Dickinson, 1972. Empirical orthogonal representation of time series in the frequency domain Part I: Theoretical considerations. *J. App. Meteor.*, 11: 887-892.
- Walsh, J. J., 1971. The relative importance of habitat variables in predicting the distribution of phytoplankton at the ecotone of the Antarctic upwelling ecosystem. *Ecol. Monogr.*, 41: 291-309.
- Walsh, J. J., 1972. Implications of systems approach to oceanography. *Science*, 176: 969-975.
- Walsh, J. J., 1975. A spatial simulation model of the Peru upwelling ecosystem. *Deep-Sea Res.*, 22: 201-236.
- Walsh, J. J., 1976. A biological sketchbook for an eastern boundary current, in *The Sea*, Vol. 6, J. H. Steele, J. J. O'Brien, E. D. Goldberg, and I. N. McCave, eds., Wiley Interscience, New York, in press.
- Walsh, J. J., J. C. Kelley, R. C. Dugdale, and B. W. Frost, 1971. Gross biological features of the Peruvian upwelling system with special reference to possible diel variation. *Inv. pesq.*, 35: 25-42.
- Walsh, J. J., J. C. Kelley, T. E. Whitley, J. J. MacIsaac and S. A. Huntsman, 1974. Spin-up of the Baja California upwelling ecosystem. *Limnol. Oceanogr.*, 19: 553-572.